NO_x generation by atmospheric air transient spark for biomedical applications

M. Janda[1], K. Hensel[1], V. Martišovitš[1], Z. Machala[1]

[1]*Division of Environmental Physics, Faculty of Mathematics, Physics and Informatics*
Comenius University, Mlynská dolina F2, Bratislava 84248, Slovakia

Atmospheric pressure air discharges often generate nitrogen oxides, especially at higher gas temperatures in the plasma. Transient spark (TS) is a DC-driven self-pulsing discharge with short duration (~10-100 ns) high current pulses (>1 A), with the repetition frequency 1-10 kHz. Thanks to the short spark duration, highly reactive non-equilibrium plasma is generated, producing ~300 ppm of NO_x per input energy density 100 $J.l^{-1}$. Further optimization of NO/NO_2 production to improve the biomedical/antimicrobial effects is possible by modifying the electric circuit generating the TS. The precursors of NO_x production and the temperature in TS were studied by nanosecond time-resolved optical diagnostics: photomultiplier module and iCCD camera coupled with spectrometer.

1. Introduction

In the past few years, plasma community witnesses a fast development of biomedical applications of cold atmospheric plasmas, since cold plasmas provide multiple agents that can efficiently kill bacteria and other hazardous microbes, and cause multiple biomedical and therapeutic effects in higher organisms. It is very important to assess the role of the plasma agents involved. At present, the major role in atmospheric pressure plasmas generated in air is typically attributed to reactive oxygen and nitrogen species (RONS) [1, 2].

The aqueous RONS are formed from dissolved NO, NO_2, O_3, and OH radicals generated by plasma in the gas phase. The first step in the optimization of water bio-decontamination process is thus better understanding of the NO and NO_2 generation in the gas phase. This problem has already been partially addressed by authors in exhaust gas cleaning applications by electrical discharges [3-6]. However, they mostly studied NO reduction, or its oxidation to NO_2, and finally to HNO_3. A recent paper [7] investigated the NO and NO_2 formation and their bactericidal effects in hybrid glow-spark discharges in air. Here we present a study focused on the synthesis of NO, NO_2 and their precursors (O and N radicals) by the transient spark (TS) discharge in air.

2. Experimental set-up

The experiments focused at optical diagnostics of TS were carried out in ambient air. The air flow velocity was about 0.2 $m.s^{-1}$, perpendicular to the inter-electrode axis. The distance *d* between the steel electrodes (point-to-point configuration with anode at the top) was 4-7 mm. The electrodes were made of a 2-mm diameter rod. The anode tip was sharpened whereas the cathode was blunt. The curvature radius of the anode tip was of the order of 100 μm. The curvature radius of the cathode was of the order of a millimeter.

For the experiments focused at the NO_x production, the electrodes were placed in a closed tube with two valves for the gas inlet and outlet. These experiments were carried out in synthetic air from the pressure tanks (N_2:O_2 = 4:1, N_2: 99.99% purity, O_2: 99.5% purity), with flow rate 1.3-2.6 $l.min^{-1}$. We used a gas analyzer Kane KM9106 Quintox to measure the gas composition after passing through the discharge reactor. It can detect NO and NO_2 in the range of 0-1000 ppm with an accuracy of 3 %.

A dc HV power supply connected to the anode via a series resistor (R = 4.92 - 9.84 MΩ) was used to generate a positive TS discharge. The discharge voltage was measured by a HV probe Tektronix P6015A and the discharge current was measured on a 50 Ω or 1 Ω resistor shunt. Electric signals were recorded by a 200 MHz digitizing oscilloscope Tektronix TDS2024.

For fast recording of time-integrated broadband spectra (200 - 1100 nm), we used a two-channel compact emission spectrometer Ocean Optics SD2000 (spectral resolution 0.6-1.7 nm). The time-resolved emission spectra were obtained using a 2-m monochromator Carl Zeiss Jena PGS2 (spectral resolution 0.04-0.09 nm, depending on the entrance slit opening), covering the UV and VIS regions (200 - 800 nm), coupled with an intensified CCD camera Andor Istar (2 ns minimum gate).

The iCCD camera was triggered by a 5 V rectangular pulses generator with less than 5 ns rise time. This generator was triggered directly by the discharge current signal, causing an additional delay of less than 10 ns. This delay, plus the delay caused by the transmission of the signal by BNC cables, was compensated by using a 10 m long optical cable

(Ocean Optics P400-10-UV-VIS). When we measured with the iCCD camera, an additional small resistor r = 1 kΩ was attached directly to the anode. Its role was to eliminate the electric signals oscillations causing problems with the iCCD camera triggering (more details in [8]).

For fast measurements of the emission intensity evolution, we used a PMT module Hamamatsu H955 (2.2 ns rise time). In order to isolate a specific spectral transition for PMT measurements, a bandpass interference filter (e.g. Melles Griot 03 FIU127 for the N_2 (C-B, 0-0) transition), was inserted into the optical path. The PMT module signal was recorded using the oscilloscope. The experimental set-up is depicted in figure 1.

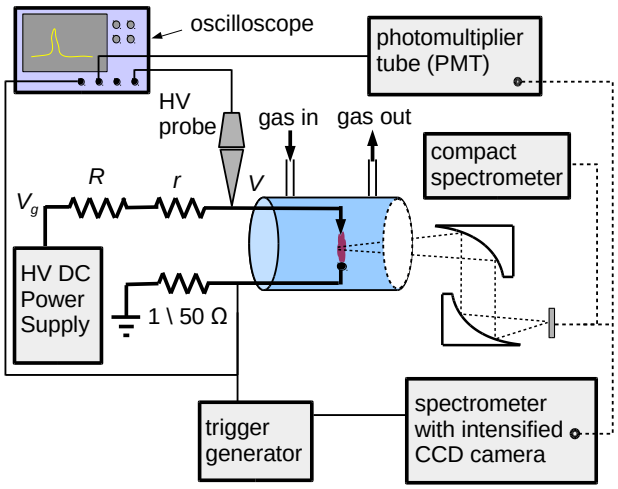

Figure 1. Simplified schematic of the experimental set-up.

3. Results and discussion

Transient spark is initiated by a streamer, when the potential on the stressed electrode V reaches voltage V_{TS}, characteristic for the TS (figure 2). The streamer forms a relatively conductive plasma bridge between the electrodes leading to the transition to spark. During the spark phase, the electric circuit internal capacity discharges completely and the voltage on the HV electrode drops to almost zero (figure 2). The discharge current reaches a high value (~1-10 A). Transition to an arc after the spark phase is restricted by the large ballast resistor R. As a result, the plasma decays after the spark pulse. Eventually, the potential V on the anode gradually increases, as the capacitor C recharges. A new TS pulse, initiated by a new streamer, occurs when the potential V reaches the breakdown voltage V_{TS} again. The TS is thus based on repetitive charging and discharging of C with the characteristic repetition frequency f in the range 1-10 kHz.

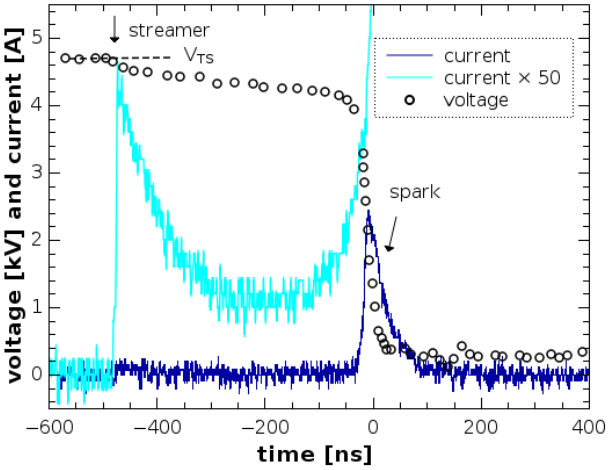

Figure 2. Typical TS voltage and current waveforms.

The time-integrated emission spectroscopy study confirmed that TS pulses generate highly reactive non-equilibrium plasma with excited atomic radicals (O^*, N^*), excited molecules N_2^* and ions N_2^{+*}. However, the TS characteristics change with increasing f, the spark pulses become smaller and broader. The emission characteristics reflect these changes. Below ~3 kHz, the atomic line emission (O^*, N^*) and molecular N_2 2nd positive system dominates in the spectra, but at higher frequencies, these atomic lines almost disappear. This might be interpreted as a decrease of the TS ability to produce radicals and to induce chemical changes at higher frequencies, but it was not confirmed by the measurement of the nitrogen oxides densities.

Due to the increasing input power, the densities of both NO and NO_2 increase with f (figure 3). However, based on the NO and NO_2 densities recalculated of per input energy density 100 $J.l^{-1}$ (figure 4), the NO generation efficiency tends to improve with increasing f, while the efficiency of the NO_2 generation decreases. The total NO_x, i.e. the sum of NO and NO_2 densities do not change significantly. These results show that the ability of TS to induce chemical changes cannot be evaluated using the total NO_x densities but it is the NO_x synthesis mechanism that changes with the increasing TS repetition frequency.

Despite the fact that TS generates 'cold' non-equilibrium plasma, there is some gas preheating between the electrodes due to increasing f [9]. We therefore have to consider the Zeldovich thermal mechanism of the NO_x generation. This mechanism is initiated by the thermal decomposition of N_2 and O_2 into their atomic states at high temperature (above ~1500 K). Next, both N and O atomic radicals are able to produce NO.

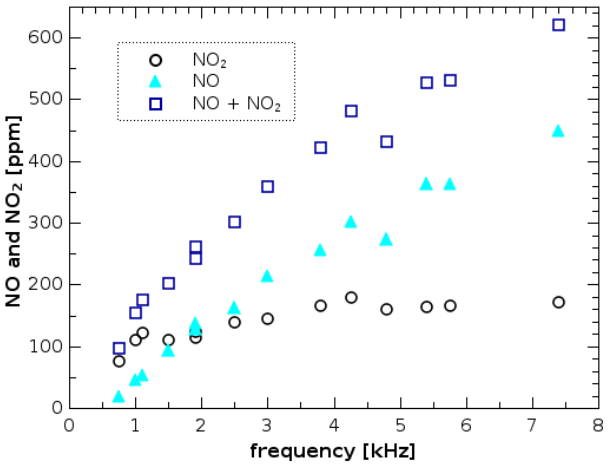

Figure 3. The NO and NO_2 densities produced by TS as functions of *f*.

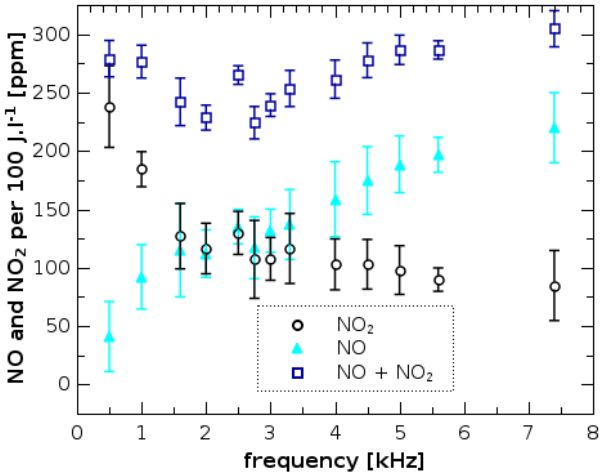

Figure 4. The NO and NO_2 produced by TS per energy input 100 $J.l^{-1}$.

The temperature at which the initiating streamer phase of TS starts (T_{str}) was only ~600 K at $f \approx$ 10 kHz (figure 5). Temperature high enough to induce thermal decomposition of N_2 and O_2 is achieved only during the spark phase of the TS (T_{spark}, figure 5). However, the thermal decomposition of N_2 and O_2 could play an important role only if the temperature remained high enough for long time after the spark.

We approximated T_{str} and T_{spark} by the rotational temperature T_r of the $N_2(C)$ species. The T_r was obtained by fitting the time-resolved (5-20 ns time window) experimental emission spectra of the N_2 2nd positive system (0-0 transition) with the simulated ones, using Specair program [10]. However, this emission can be observed only for a short time after the streamer and spark current pulses (see figures 6 and 7, respectively), so we cannot measure the entire temperature evolution between two successive TS pulses.

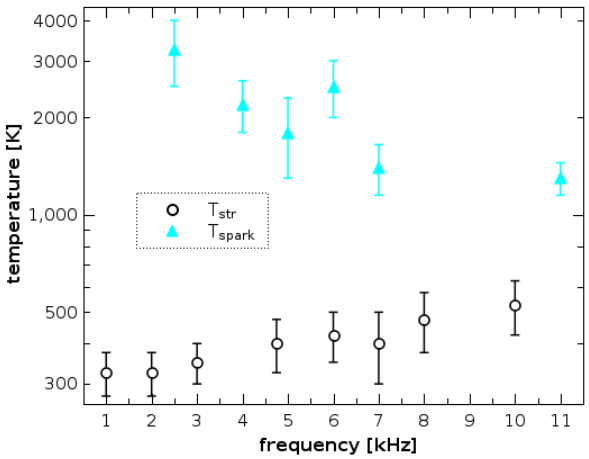

Figure 5. Temperature at the beginning of the streamer phase and the highest temperature during the spark phase of the TS as functions of *f*.

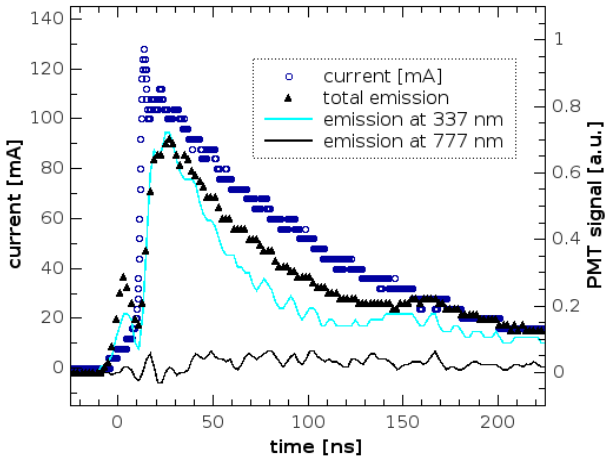

Figure 6. Typical PMT signals of the optical emission during the streamer phase of TS, $f \sim 2$ kHz.

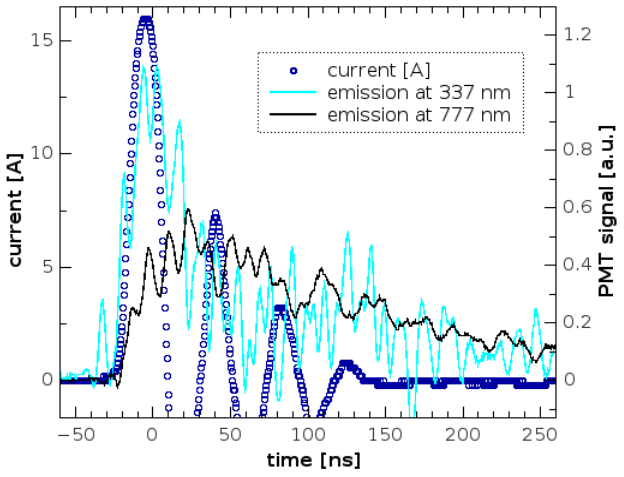

Figure 7. Typical PMT signals of the optical emission during the spark phase of TS, $f \sim 2$ kHz.

Thus, we cannot definitely asses the role of the thermal decomposition of N_2 and O_2, but we assume that other plasma processes are more important,

since the electron density is very high during the spark phase of the TS [11].

Information about these processes can be deduced from the emission profiles obtained by the PMT. The $N_2(C)$ emission starts with the beginning of both streamer and spark current pulses. During the rising slope of the current pulses, the electrons must have enough energy to ionize N_2 and O_2. We therefore assume that the majority of the $N_2(C)$ states are created by high energy electrons. The quenching of excited N_2^* molecules, such as $N_2(C)$ with molecular oxygen is probably one of the major sources of atomic oxygen.

It is necessary to mention that the O species production need not be correlated with the O^* emission intensity. The emission from the excited O^* atoms can be observed almost exclusively during the spark phase, and its peak is slightly delayed with respect to the current rising edge (figure 7). The electron mean energy after the spark current pulse is around ~1 eV corresponding to the electron temperature ~10000 K [10]. We therefore suppose that O^* atoms are not produced by high energy electrons, but via dissociative recombination of relatively slow electrons with O_2^+ ions.

This can explain why there is almost no O^* emission during the streamer – the degree of ionization is much lower compared to spark. For the same reason, the atomic line emission intensity weakens at higher TS frequencies – spark current pulses are smaller and broader, and the electron density is lower [11]. It could also explain the increase of the NO/NO_2 ratio with increasing *f*. Thanks to the dissociative recombination, there might be enough O to produce not only NO, but also further oxidize it to NO_2.

4. Conclusions

Our aim was to investigate the generation of significant biomedical and biocidal agents NO and NO_2, , by the self-pulsing Transient Spark (TS) discharge in atmospheric pressure air. In dry synthetic air, the sum of NO and NO_2 densities more than 600 ppm was achieved with power input below 6 W (~300 ppm per 100 J of energy deposited per 1 liter of gas). In future, we plan to optimize the NO_x production by varying parameters of the electric circuit (external resistor, internal capacitor, distance of electrodes).

The TS characteristics change with the increasing TS repetition frequency. These changes also influence the generation of excited atomic species and nitrogen oxides. The atomic lines emission intensity decreases and the NO/NO_2 ratio increases with increasing TS repetition frequency. We attempted to explain these changes using temporal emission intensity profiles measured by photomultiplier tube.

The excited N_2* molecules are produced by high energy electrons during the rising slope of the current pulses, both streamer and spark. These excited nitrogen molecules can lead to the sufficient atomic oxygen production necessary for the synthesis of NO. The excited atomic oxygen species are mostly produced during the spark current decreasing slope, probably via dissociative recombinations of O_2^+. This provides additional atomic oxygen for the NO oxidation to NO_2. Since the TS spark pulses are getting broader and smaller with increasing frequency, this would explain why atomic lines weaken and NO/NO_2 ratio increases with the increasing TS frequency. Further research including kinetic modelling and measurement of O species in the ground state is required to prove this hypothesis.

Acknowledgement

Effort sponsored by the Slovak Research and Development Agency APVV-0134-12, and Slovak grant agency VEGA 1/0918/15.

References

[1] D.B. Graves, *J. Phys. D: Appl. Phys.* **45** (2012) 263001.

[2] Z. Machala, L. Chládeková, M. Pelach, *J. Phys. D: Appl. Phys.* **43** (2010) 222001.

[3] B.M. Penetrante et al., *Appl. Phys. Lett.* **67** (1995) 3096.

[4] M. Dors et al., J. Electrostat. **45** (1998) 25.

[5] J.T. Herron, *Plasma Chem. Plasma Proc.* **21** (2001) 581.

[6] Zhao G-B et al., *Ind. Eng. Chem. Res.* **43** (2004) 2315.

[7] M.J. Pavlovich et al., *J. Phys. D: Appl. Phys.* **47** (2014) 505202.

[8] M. Janda et al., *Plasma Sources Sci. Technol.* **20** (2011) 035015.

[9] M. Janda et al., *Plasma Sources Sci. Technol.* **21** (2012) 045006.

[10] C.O. Laux et al., *Plasma Sources Sci. Technol.* **12** (2003) 125.

[11] M. Janda et al., *Plasma Sources Sci. Technol.* **23** (2014) 065016.